Computer Science and Information Systems 13(2):623–638 DOI: 10.2298/CSIS160224019L

A Two-step MF Signal Acquisition Method for Wireless Underground Sensor Networks

Wei Liang[1], Yong Xie[1], Xuhui Chen[1], Osama Hosam[2,3], and Xiaoyan Chen[1]

[1] Department of Software Engineering, Xiamen University of Technology,
Xiamen, Fujian 361024, China
{wliang, yongxie, xhchen, yxc}@xmut.edu.cn

[2] Computer Science and Engineering College, Taibah University,
Yanbu, Saudi Arabia
mohandesosama@gmail.com

[3] The City for Scientific Research and Technology Applications,
IRI, Alexandria, Egypt

Abstract. Signal acquisition plays a critical role on the bit error rate (BER) of a direct sequence spread spectrum (DS/SS) communication system working with low frequency. In this paper, we propose a new signal acquisition method. The acquisition process includes coarse matched filter (MF) location in the first stage and an accurate MF acquisition as a verification mode for the second stage. The performance metrics, including mean acquisition time (MAT) and power consumption, are accuracy. The results indicate that when the signal-to-noise ratio (SNR) keeping consistent, the MAT of the proposed method is less than the original one. When the SNR is around -5dB, the system mismatch rate is about 5.6×10^{-4}, which takes only one percent of those achieved in the original acquisition algorithms. The two-step MF acquisition method is stable except its power consumption being a little higher than the original method.

Keywords: acquisition, spread spectrum, signal processing, wireless communication, underground sensor networks.

1. Introduction

Wireless underground sensor networks (WUSNs) is currently a fairly active and promising research field. It can be applied to determine locations and monitor a variety of conditions, such as soil properties for agricultural applications and toxic substances for environmental monitoring [16][5][30]. However, there are still a large amount of challenges when WUSNs are applied to underground environment. There are factors, such as extreme path loss, reflection/refraction, multi-path fading, reduced propagation velocity and ambient noise, impact the reliability of underground communication with the electromagnetic (EM) waves [8][27].

Spread spectrum communication is an efficient solution for supporting underwater acoustic communication [28], owing to its characteristics of anti-interference, anti-multipath fading [9], Doppler shift compensation with phase synchronization, effective utilization of bandwidth, and easy implementation of code division multiple access (CDMA). However, in actual underwater acoustic communication systems, the signal-to-noise ratio (SNR) of spread spectrum's input signals is relatively low. Therefore, signal acquisition, i.e. capturing signals accurately and synchronizing them in communication chips, is critical, for the entire system's bit error rate (BER) is directly affected by the capture position. Signal acquisition plays a vital role in signal processing. It can be used to decide the exact division of useful data and preamble. With the development of rapid Pseudo-Noise (PN) code acquisition with matched filter (MF) in a DS/SS system, a lot of targeted methods have come into use. For example, in order to solve the acquisition in DS/SS with a large frequency offset, paper [21] proposes a method dividing MFs into a series of sets to correspond to partial sequences of the PN code. Aiming at a frequency-hopping DS/SS system, parallel acquisition with MF can improve performance of MAT when involving more branches of parallelism [4]. Meanwhile, by using MF with multi-vaues coefficients, we can assure whether the acquisition is established or not within a shorter duration [29]. In addition, two methods are proposed to solve the problem of Doppler frequency shifting. The first one involves a segmented transversal matched filter (SMF) acquisition which is suitable for personal communications systems [23]. The other one gives us the improved SMFs with FFT approach. This method realizes fast acquisition in premise that Doppler shifts considered, however, larger power consumed. Lots of researches on applying signal acquisition to different environments, such as asynchronous cellular networks [17], impulse radio ultra wide band systems (IR-UWB) [25], coherent optical pulse CDMA [10],LEO mobile satellite communications have been considered [15] [14].

The remainder of the paper is organized as follows. Section 2 illustrates and compares existing methods. The architecture of this system and the test platform is introduced in Section 3. Section 4 describes in detail the new signal acquisition method based on the MF acquisition method. This section introduces the two-step MF method in acquisition rules and acquisition theory, respectively. Section 5 evaluates this new signal acquisition scheme in MAT, BER and energy consumption. Section 6 makes a conclusion of this paper and discusses the directions for future work.

2. Related Work

A variety of classical signal acquisition methods are shown in this paper, such as serial signal acquisition [22], sequential estimation [11], parallel signal acquisition [18] and MF signal acquisition [26]. In this section, we have summarized previous schemes of signal acquisition and analyzed the performance.

Serial search is based on shifting the receiver code, which is relative to the incoming waveform in discrete steps. This method keeps searching until a preset threshold is exceeded. For example, Dicarlo and Weber [7] present N-dwell serial acquisition method, which uses multiple dwell procedures to reduce the expected acquisition time obtained with a single dwell system. Puska et al. have investigated three serial search code acquisition methods for DS/SS systems utilizing smart antennas. It is sensitive to interference and offers short mean acquisition times using different antennas [24]. However, the search speed usually has hardware delay, even though using simple hardware circuits [6]. Sequential estimation decreases the mean acquisition time (MAT) except for overcoming high co-user noise. Meanwhile, in order to improve the performance of MAT, [12] introduces a method combining MF with serial search. Unfortunately, it is still unable to handle phase rotations due to Doppler shifts. Parallel search is prone to having a higher mismatch rate than the MF method, for instance, Kong and Nam have studied a parallel search acquisition method which achieve small delay performance [19]. However, parallel search occupies more resources than serial and MF schemes, which directly leads to high power consumption. The authors in [31] propose a robust MF acquisition to eliminate the cases of false alarm in signal acquisition. It significantly improves performances over the conventional matched-filter algorithm for the specific UWB channel model. A compact digital matched filter (DMF) acquisition system is proposed in [13], which achieves a mean acquisition time comparable to that of the conventional DME. However, it allows an unlimited period of integration and some advantages in terms of probabilities of detection and false alarm. Therefore the proposed DMF requires a short device length and still provides a fast acquisition. [20] proposes a low-power 128-tap dual-channel direct-sequence spread-spectrum (DSSS) digital matched-filter chip. It adopts a double-edge-triggered clocking scheme. The experiments show it has low power consumption and can be used for code acquisition of DSSS signals in portable systems.

Because of the MF method having a better performance than others, this paper proposes a two-step signal acquisition method based on the MF scheme, which can typically apply to wireless underground sensor networks (WUSN). Our aim is to provide a state-of-the-art signal acquisition method for WUSN which has been examined in terms of the accuracy of signal acquisition, BER, power conservation, and additional features.

3. Architecture

The architecture generally includes some well-known components of any wireless communication system, such as channel coding, interleaving, spread, carrier modulation and bandpass filter at the sender respectively. In receiver, signal acquisition, de-spread, carrier de-modulation, channel decoding, bandpass filter, low-pass filter and receiving antenna are included at the receiver. All parts are illustrated in Fig.1.

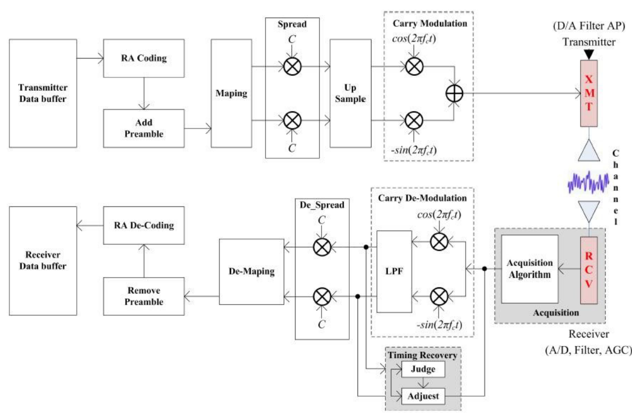

Fig. 1. The architecture of the low-frequency communication system for WUSNs

The core in this paper is signal acquisition which is the first thing needed to be done at the receiver. Signal acquisition plays a critical role in the division of the preamble and useful data. The specific method is depending on the spread scheme and the concrete applications it will be applied to. In order to increase the SNR, doing the correlative calculation before carrier de-modulation is a good choice to get the shot of the useful data, which is also named as MF signal acquisition. Therefore, signal acquisition must be put in front of the carrier de-modulation and de-spread while processing the received data. Besides, we prefer to give a new proposal based on the MF signal acquisition.

The low-frequency communication test platform is presented in Fig.2. It primarily includes a processor [1], field-program gate array (FPGA) [2], ADDA [3] and daughter boards that represent RF front ends of receiver and transceiver. The dominant part of the system is FPGA being responsible for the digital logic implementation of signal processing algorithms. Before the test, we download the related signal processing algorithms of the whole architecture into the FPGA through the JTAG interface. The signal acquisition is a vital composition while processing the received data. Considering the strong ambient noise in underground channel, it is necessary to adopt the direct sequence spread signal processing method to increase the range frequency spectrum in order to make the SNR as large as possible.

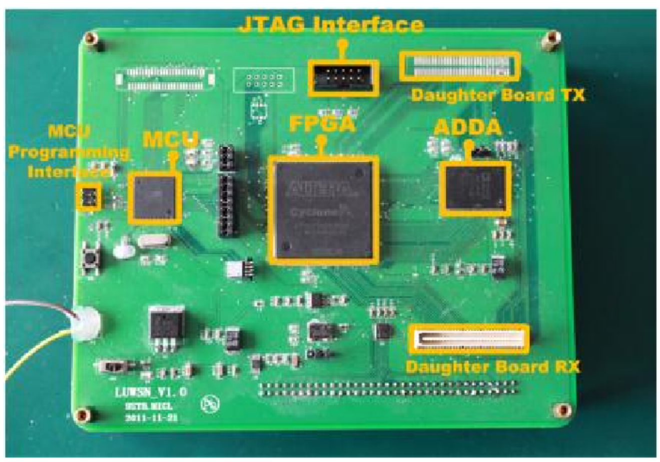

Fig. 2. Hardware platform for WUSNs

4. Two-step MF Signal Acquisition Method

For ease of reading, this statement of new approach will be divided into two subsections. Firstly, according to acquisition rules, the scheme of the new acquisition method will be introduced. Then, the introduction of capture theory and the threshold range model follows.

4.1. Acquisition Rules

As shown in Fig.3, the received signal goes through the MF two times. In the former one, the MF is applied to the whole spread code. The output signal of the filter is proportional to the autocorrelation function (ACF). It is assumed that the ACF has zero value except in the case that the code is completely inside the filter whose value of ACF is one. Then, the outputs of the MF access the comparator. The comparator uses the threshold T_h in a way that the output shows "1" (hit), if $x(t) \geq T_h$, and "0" otherwise. Here, $x(t)$ is the input signal. Thus we can roughly determine the capture point in the first step. Then, set this point as the right endpoint and regard the length of preamble after coding as the interval length. In the second instance, the MF is applied to this interval. Meanwhile, set a higher sampling rate at the matching filter compared to the first step. Comparators are used in both steps. However, T_h changes with the sample rate. Analysis will be shown in the second subsection. By selecting each of the two-step sampling rates under premise of balance capture accuracy and real-time performance, we can reach an accurate capture point. If the sample rate is low, the false alarm P_{fu} [25] is catastrophic and causes a total miss of the correct code phase. On the contrary, the higher sample rate will increase the MAT and power consumption. Thus, a proper balance sample rate is a key for two-step.

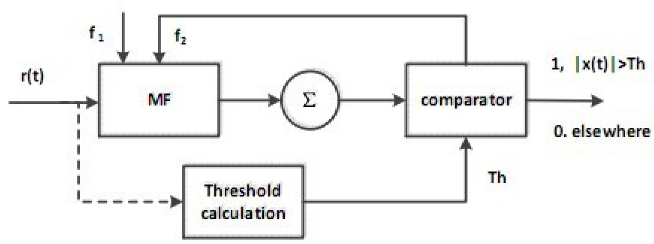

Fig. 3. The scheme of two-step MF acquisition

4.2. Acquisition Theory and the Threshold Range Model

Signal acquisition algorithm uses relationship between sampled data and the copies of spread digital waveforms to compute correlation values and find out the synchronization position. Amount of certain standard spread digital waveforms are designed as the preamble to implement. The source information is converted into binary digits. The pseudo-random sequence, i.e., the Gold codes with good auto correlation and cross correlation, is adopted to realize spread spectrum in this paper. Assume that the length of Gold codes is K, the sampling rate of a sinusoid is M, then one original data bit will be $K \times M$ digital waveform samples after spectrum spread and modulation. The length of the acquisition window is set as $L = K \times M$, which can be modified to other values during simulation. In receiver, the sampled digital waveform $r(t)$ enters the acquisition window. It performs correlation operation with a modulated local spreading code vector $h = [h_0, h_1, \cdots, h_{L-2}, h_{L-1}]^T$, which is stored in matched filters. When K waveform samples slide through the acquisition window, the K correlation values are buffered by the comparator. Comparator selects the maximum value and gives the synchronous position of the corresponding waveform sample.

The sequence of binary digits spread by Gold Coding is a bit stream $s_g(t)$ can be expressed as (1):

$$s_g(t) = c(d(t)) \tag{1}$$

Here, $d(t) \in \{0,1\}$ is the original data bit and $c(\cdot)$ is the Gold sequence expansion. Thus we have $s_g(t) \in \{0,1\}$. Assuming $s_g(t)$ has K digits, the modulated transmitting signal $s(t)$ is defined as (2):

$$s(t) = \Re\{s_g(t)e^{j2\pi kt/T}\} \tag{2}$$

Here, T represents the transmitted period, k stands for the carrier frequency and $\Re$ indicates the real part of a complex number. We assume that the received signal waveform $r(t)$ to be

$$\begin{aligned} r(t) &= s(t) * h(t) + N(t) \\ &= \sum_{n=0}^{N-1} s(t_n)h(t-t_n) + N(t) \\ &= \sum_{n=0}^{N-1} s_n h(t - nT - \varepsilon_n) + N(t) \end{aligned} \tag{3}$$

Where $h(t)$ is the channel's impulse response, $t_n = nT + \varepsilon_n$ represents the $n-th$ time period, ε_n is the timing offset for the $n-th$ symbol, and $N(t)$ is Gaussian noise. We assume that ε_n is a random walk, i.e., $\varepsilon_n = \varepsilon_0 + \sum_{i=0}^{n-1} \upsilon_i$, where ε_0 is the initial phase, υ_i is an independent random variable with mean to be 0 and variable to be σ^2. Thus it is easy to derive that ε_n has mean value ε_0, variance $n\sigma^2$ and t_n has mean value $nT + \varepsilon_0$ and variance $n\sigma^2$, i.e. $\varepsilon_n \,\tilde{}\, N(\varepsilon_0, n\sigma^2)$ and $t_n \,\tilde{}\, N(nT + \varepsilon_0, n\sigma^2)$.

The stability of a system is an important property that we have to consider in practical implementations. In this paper, we assume the impulse response is a summation of absolute value, i.e.,

$$S_h = \sum_{n=-\infty}^{\infty} |h(n)| < \infty \tag{4}$$

In this condition the output $r(t)$ is almost bounded. Since $s(t) \leq M$ for some M, we have

$$r(t) \leq M \sum_{n=0}^{N-1} |h(t-t_n)| + |N(t)| < \infty + |N(t)| \tag{5}$$

Then, it is sampled by an impulse train as the input signal for the receiver. We are now ready to describe how to implement the acquisition in the first matched filter. Here we assume that both the transmitting and receiving's clocks keeping same during the progress. That is, there is no frequency change between transmitter and receiver. Denote the sampled signal by $r_s(t)$, thus

$$r_s(t) = r(t) \tag{6}$$

The ideal sampling time to the signal waveform $r(t)$ begins when $r(t)$ just reached the receiver. However, it is difficult to achieve in practice. It is necessary to design a method of obtain signal's starting edge before the signal arrival in receiver. Due to the unpredictable noise and phase shift, we have to choose one method to decide the first signal waveform of $r(t)$. Let the real sampled signals be $r_R(t_0), r_R(t_1)$, $r_R(t_2), r_R(t_3), r_R(t_4), r_R(t_5)$,... . We shall call it l-sample if $r_R(t_l) = r_s(t_0)$ representing the correct signal being sampled at time l. As sampling of the signal is done before $r(t)$ arrives at the receiver, $r_R(t_k)$ is interfering noise signal when $k < l$ and it is l-sample.

Assume the correct preamble, denoted by $P = \{p_0, p_1, \cdots, p_{L-1}\}$, has L digits. Then the data storage matrix, denoted by $W \in R^{k \times L}$ with $k \geq L$, is

$$\begin{aligned} W &= \begin{bmatrix} r_{0,0} & r_{0,1} & \cdots & r_{0,L-1} \\ r_{1,0} & r_{1,1} & \cdots & r_{1,L-1} \\ \vdots & \vdots & \ddots & \vdots \\ r_{k-1,0} & r_{k-1,1} & \cdots & r_{k-1,L-1} \end{bmatrix} \\ &= \begin{bmatrix} r_R(t_{L-1}) & r_R(t_{L-2}) & \cdots & r_R(t_0) \\ r_R(t_L) & r_R(t_{L-1}) & \cdots & r_R(t_1) \\ \vdots & \vdots & \ddots & \vdots \\ r_R(t_{k+L-2}) & r_R(t_{k+L-3}) & \cdots & r_R(t_{k-1}) \end{bmatrix} \end{aligned} \tag{7}$$

If the sampling is l-sample, the data in the first $l-1$ rows are all noise signals. To verify the position of $r_s(t_0)$, we use the cross-correlation to generate k cross-correlation values. It is denoted by R_{WP} between W and P, i.e.,

$$\begin{aligned} R_{W_iP}(0) = W(0) * P(0) &= \sum_{n=0}^{L-1} r_{i,n} p_n \\ &= \sum_{n=0}^{i-l+1} r_{i,n} p_n + \sum_{n=i-l}^{L-1} N p_n \end{aligned} \tag{8}$$

Since N represents noise signal, we consider it has little influence on this cross-correlation, that is, the expected value of Np_n is very small, more precisely, $E(|Np_n|) \leq e$, where e is the zeroth order error. Thus,

$$\begin{aligned} R_{W_iP}(0) &= \sum_{n=0}^{i-l+1} r_{i,n} p_n + (L-i)e \\ &\approx \sum_{n=0}^{i-l+1} r_{i,n} p_n = \sum_{k=0}^{i-l+1} r_R(t_k) p_k \\ &= \sum_{k=0}^{i-l+1} [\sum_{n=0}^{N-1} s_n h(t - nT - \varepsilon_n) + N(t)] p_k \end{aligned} \tag{9}$$

One may incorrectly conclude that the cross-correlation is non-decreasing with the growth of the quantity of same elements between W and P. In fact, all transmitted data moves one step when a time interval increases, which deduces all the pairs of corresponding data between W and P. They are different from the case in the previous time. The maximum cross-correlation takes place when the exact preambles are totally sampled by the receiver. All of the data from the transmissions keep exactly same with the preambles P. The theoretical maximum (when considering small noise) is derived as below.

$$\omega = \max_{i=0}^{k}\{R_{W_iP}(0)\} = \max_{i=0}^{k} < W_i, P > \approx \|P\|_2 \tag{10}$$

Here $< x, y >$ represents the inner product on x and y, $\|x\|_2$ represents Euclidian 2-norm of x, i.e., $\|x\|_2 = (x_1^2 + x_2^2 + \ldots + x_n^2)^{\frac{1}{2}}$. However, when noise is strong, the influence of transmitted signal is substantial and the actual maximum cross-correlation will be larger than the theoretical threshold.

Since transmitting signal is interfered by noise, there exists random factors in this model, i.e., the time offset ε_n and Gaussian white noise $N(t)$. To analyze the statistical properties of the model, we assume the impulse response to be

$$h(x) = e^{-x} \tag{11}$$

This function has several good properties in probability. We can obtain that the impulse response is an absolutely summation we expected for. The results may be different if other impulse response functions are chosen. The impulse response is

$$h(t - nT - \varepsilon_n) = e^{-t+nT}e^{\varepsilon_n} \tag{12}$$

Thus the random factor moves to an exponential random variable whose logarithm is normal distribution. This random variable is log-normal distributed in probability. As we mentioned before, $\varepsilon_n\tilde{}N(\varepsilon_0, (\sqrt{n}\sigma)^2)$, that is, ε_n is normally distributed with an expected value of ε_0 and standard deviation of $\sqrt{n}\sigma$. Referring to the log-normal variable e^{ε_n}, the expected value and variance are

$$\begin{aligned} E(e^{\varepsilon_n}) &= e^{\varepsilon_0 + \frac{1}{2}n\sigma^2} \\ Var(e^{\varepsilon_n}) &= e^{2\varepsilon_0 + n\sigma^2}(e^{n\sigma^2} - 1) \end{aligned} \tag{13}$$

We can obtain that the variance increases as n increases. The other random factor is Gaussian noise $N(t)$, which is normally distributed with expected value 0 and variance σ_g^2 at any time t. Consequently, due to the fact that the two random factors are independent, we can combine these two random factors as follows,

$$\sigma_m = \sqrt{e^{2\varepsilon_0 + n\sigma^2}(e^{n\sigma^2} - 1)} + \sigma_g \tag{14}$$

Furthermore, to verify whether the maximum of cross-correlation does represent all preambles that have been sampled, we introduce a statistical inference approach. The expected theoretical maximum value of cross-correlation is $\|P\|_2$, the standard deviation is σ_m. In 95% confidence interval, the value of cross-correlation we calculated should be in the interval

$$[\|P\|_2 - 1.96\sigma_m, \|P\|_2 + 1.96\sigma_m] \tag{15}$$

If σ_m is much smaller than $\|P\|_2$, the lower bound $\|P\|_2 - 1.96\sigma_m$ is not far from $\|P\|_2$. In this case, if all the preambles are sampled, the lower bound can be acted as a pre-setting threshold. However, if σ_m is not sufficiently smaller than $\|P\|_2$ or even larger than $\|P\|_2$, it leads to the lower bound be nearly 0 or negative. In such situation, the lower bound has no practical significance. This lower bound is no longer an appropriate threshold, since signal can be interfered by small noise at any time. Hence, we must keep cross-correlation value beyond the lower bounds. Besides, we can get from (15) that sample rate decides the value of $\|P\|_2$. Therefore, although this two-step comparator principle is same, the threshold varies with the changes on sampling rate.

5. The Numerical Results

We assume the length of the preamble is n bits. After spreading and sampling, the length of preamble is $n \times K \times M$. We first add the White Gaussian noise to the sending signal when simulating. Under the circumstance, the higher the defined sampling rate is, the closer location we can find to the acquisition position. If the defined sampling rate is high, the sinusoidal wave form will be more accurately. Meanwhile, the interval of the second step achieves a greater chance of covering the true capture point. However, an extremely high sampling rate leads to resource overhead and time consumption. In a low-frequency underground communications system, transmission power should be as small as possible in order to guarantee the energy supply. This results in a dilemma between accuracy of signal acquisition and resource consumption. It is necessary to balance the sampling rate and resource consumption.

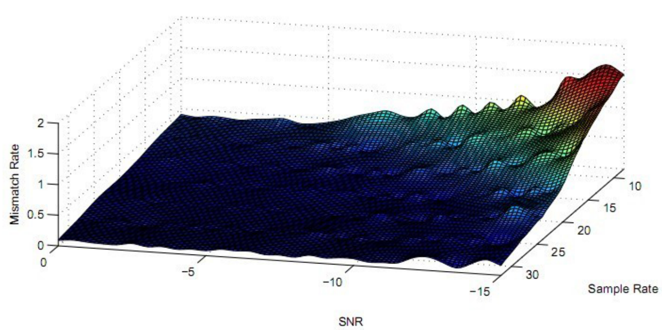

Fig. 4. The relationships among threshold, mismatch rate and SNR

Fig. 4 illustrates the relationships among sample rate, mismatch rate and SNR. The mismatch rate has negative proportion relationships with SNR and the defined sample rate. Assume the sample rates for each steps to be M_1= 16, M_2= 20, and the length of spreading code is K=7, the acquisition window length is defined as 112 and 140 to constrain the possible value corresponding to the maximum, especially for the channel with high noise and signal attenuation. Fig.5 evaluated the performance of the original MF method and two-step MF method in terms of MAT.

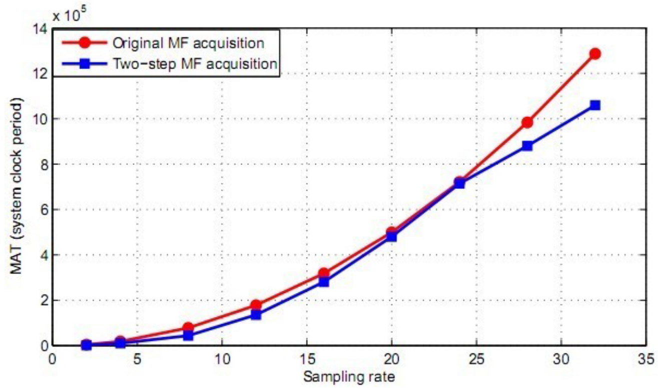

Fig. 5. The relationship among original acquisition and two-step MF acquisition in MAT

When coarse sampling rate is 16 points per period in the first step of two-step MF acquisition, we obtain better results by the new method through a large number of simulations. Hence, we suggest to set the maximum coarse sampling rate to be 16 points per period. The result in Fig.5 indicates that when the sampling rate is less than 16, the coarse sampling rate is the previous value in abscissa. For example, if the abscissa value is 12 in Fig.5, the new method of coarse sampling rate is 8. When the sampling rate is greater than 16, the new method of coarse sampling rate is determined as 16. Fig.5 shows that the time consumption of the two methods will go up monotonically with the increasing sampling rate, but the time consumption of the new method will be much less than the original one. According to n-th Lagrange Interpolation Polynomial, an n-th remainder term or bound for the error is presented as

$$R(x) = f(x) - p(x) = \frac{f^{(n+1)}(\xi(x))}{(n+1)!}(x-x_0)(x-x_1)\cdots(x-x_n) \tag{16}$$

where $f(x)$is an ideal continuous sine function of L^2 space, $p(x)$ is sine function which goes by Lagrange polynomial fitting after sampling, $(x_0, x_1, \cdots, x_n)$ are $n+1$ distinct numbers and $\xi(x)$ is a number given by the Generalized Rolle's Theorem, which satisfying $\xi(x) \in (a, b)$. For interpolation sampling theorem, $n = 1$, that means, use a line connecting two sampling point, then,

$$R(x) = \frac{f^{(2)}(\xi(x))}{2}(x-x_0)(x-x_1) \tag{17}$$

We can see $f^{(2)}(\xi(x))$ will influence the variation of $R(x)$. Since $f(x)$ is a continuous function, $f \in C_n$, that means, f is n-order differentiability, so $|f^{(2)}| < \infty$, assuming $\max|f^{(2)}| = 2c$, then

$$R(x) \leq c(x-x_0)(x-x_1) \tag{18}$$

From the above discussion, we can control the variation of $(x-x_0)(x-x_1)$ through modulate sampling frequency. In a certain range, if sampling frequency increases, sampling points in each cycle will increase, $(x-x_0)(x-x_1)$ will decrease, then $R(x)$ will also decrease and the accuracy increases. Of course, this will remain true as long as both transmitter and receiver clocks are fully synced.

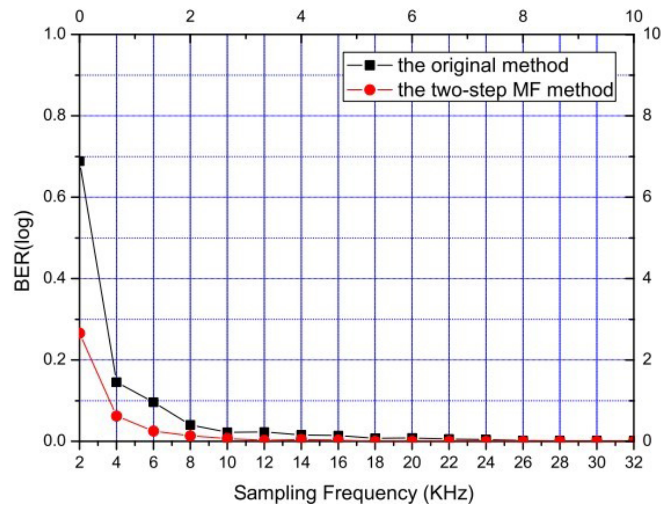

Fig. 6. The relationship among original acquisition and two-step MF acquisition in Gaussian noise channel

Fig. 6, Fig.7 and Fig.8 are BERs of the two-step method and the original method in Gaussian noise, Rayleigh noise and impulse noise respectively. In the condition of SNR being -10 and system frequency being 1 KHz, the BER of the two-step method is lower than the original method. After the Matlab simulation, we implement the algorithm by means of hardware logic design using Verilog HDL on the FPGA.

We also analyze the resource consumption by means of hardware logic design using Verilog HDL on the FPGA. We make an evaluation of the resource consumption among this new two-step MF acquisition method, the serial acquisition and original MF acquisition, especially the thermal power dissipation (TPD) and the logic elements (LEs) and memory bits, which is indicated in the Fig.9 and Fig.10. From the evaluation results we can conclude that the serial method occupies more resources than others, and the two-step method has a little larger power consumption than the original acquisition method.

6. Conclusion

In this paper, through the theoretical derivation of the threshold range, we compare the new method with the serial acquisition and the original MF acquisition in Gaussian noise channel, Rayleigh noise channel and Impulse noise channel. As shown in the paper, the two-step MF acquisition method is more advantageous over the other two methods in terms of MAT and accuracy. The maximum coarse sampling rate is 16 points per period in this two-step MF method. Especially, when sampling rate is less than 16, the BER is

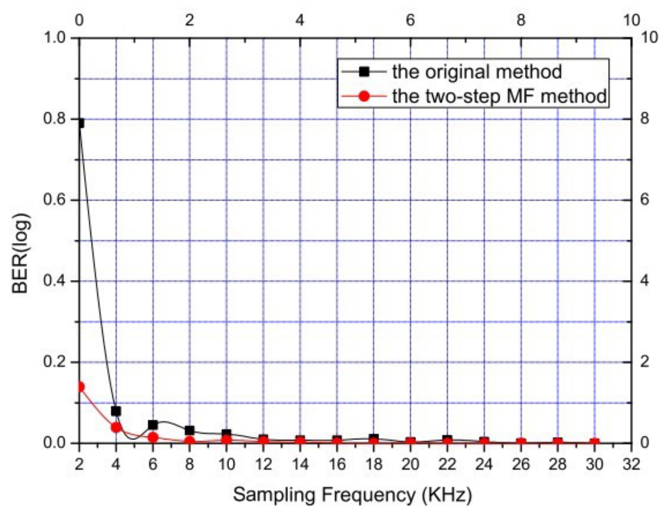

Fig. 7. The relationship among original acquisition and two-step MF acquisition in Rayleigh noise channel

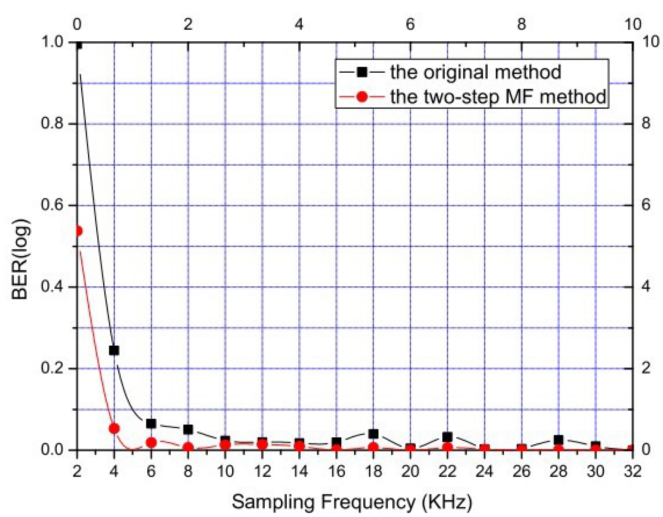

Fig. 8. The relationship among original acquisition and two-step MF acquisition in Impulse noise channel

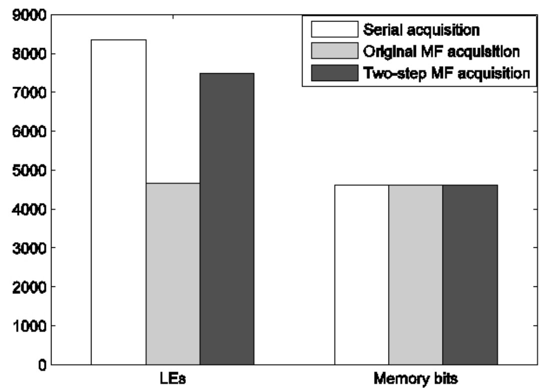

Fig. 9. The relationship on the LEs and Memory bits among the serial method, original MF acquisition and two-step MF acquisition method

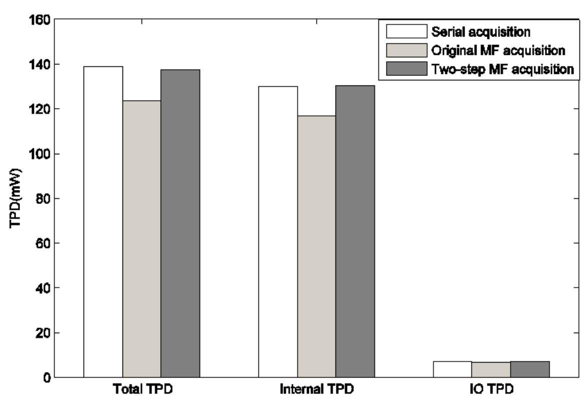

Fig. 10. The relationship on the TPD among the serial method, original MF acquisition and two-step MF acquisition method

significantly lower. There is also much future work to be considered, such as: (1) Energy efficiency. More attention will be paid to the energy efficiency on our further research considering high efficient algorithms. (2) The scope of applications. This paper describes the performance of the low-frequency communication system that is applied to underground wireless communication networks (UWCN). This system could also be applied to any other low frequency applications in the future to verify the performance of the acquisition proposed in this paper.

Acknowledgement. This work is supported by the National Nature Science Foundation of China (Grant61572188, 61502405), the Research Project supported by Xiamen University of Technology (YKJ15019R), Xiamen science and technology research project (3502Z20133033), the Science and technology project of the State Planning Commission (WKJ-FJ-35).

References

1. Atmega embedded processors and sigma dsp audio processors, [Online]. Available: http://www.analog.com/en/products/processors-dsp/blackfin.html
2. Cyclone v gx fpgas with 3.125 gbps provide the lowest system cost and power, [Online]. Available: https://www.altera.com/products/fpga/arria-series.html
3. Differential amplifiers from analog devices are highly integrated and optimized for differential signaling applications. adda, [Online]. Available: http://www.analog.com/en/index.html
4. Chau, Y.A., Joe, S.Z.: Parallel acquisition with matched filters for frequency-hopping signals. In: IEEE 4th International Symposium on Spread Spectrum Techniques and Applications Proceedings. pp. 756–760. IEEE, Mainz, USA (1996)
5. Chaudhary, D.D., Nayse, S.P., Waghmare, L.M.: Application of wireless sensor networks for green house parameters control in precision agriculture. International Journal of Wireless Mobile Network 3(1), 140–149 (2011)
6. Davisson, L.D., Flikkema, P.G.: Fast single-element pn acquisition for the tdrss ma system. IEEE Transactions on Communications 36(11), 1226–1235 (1988)
7. Dicarlo, D., Weber, C.: Multiple dwell serial search: performance and application to direct sequence code acquisition. IEEE Transactions on Communications 31(5), 650–659 (2008)
8. Elleithy, A., Liu, G., Elrashidi, A.: Underground wireless sensor network communication using electromagnetic waves resonates at 2.5 ghz. Journal of Wireless Networking and Communications 2(6), 158–167 (2012)
9. Freitag, L., Stojanovic, M., Singh, S., Johnson, M.: Analysis of channel effects on direct-sequence and frequency-hopped spread-spectrum acoustic communication. IEEE Journal of Oceanic Engineering 26(4), 586–593 (2001)
10. Huang, W., Andonovic, I., Tur, M.: Code acquisition in coherent optical pulse cdma systems utilizing coherent correlation demodulation. IEEE Transactions on Communications 48(4), 611–621 (2000)
11. Jayaweera, S.K., Hakim, K.: A cooperative game theoretic solution for lifetime maximization of wsns in sequential estimation. In: 2010 5th International Conference on Information and Automation for Sustainability (ICIAFs). pp. 233–238. IEEE, Colombo (2010)
12. Jiang, X., Yin, Z., Cui, K., Yin, L., Wu, Z.: Communication performance analysis of tdrs system ma service. In: 2014 12th International Conference on Signal Processing (ICSP). pp. 1659–1664. IEEE, Hangzhou (2014)
13. Jo, G.D., Chang, S.H., Kweon, H.Y., Kim, S.Y.: A compact matched filter for rapid code acquisition. vol. 50, pp. 713 – 717 (1999)
14. Kang, B.J., Park, H.R., Han, Y.: Hybrid acquisition in ds/cdma forward link. In: IEEE 47th Vehicular Technology Conference. pp. 2123–2127. IEEE, Phoenix, AZ (1997)

15. Kim, J.Y., Lee, J.H.: Code acquisition of a ds/cdma system with imperfect power control for leo mobile satellite communications. In: IEEE 48th Vehicular Technology Conference. pp. 1543–1547. IEEE, Ottawa (1998)
16. Kone, C.T., Hafid, A., Boushaba, M.: Performance management of ieee 802.15.4 wireless sensor network for precision agriculture. IEEE Sensors Journal 15(10), 5734–5747 (2015)
17. Kong, S.H., Nam, W.: A-gnss sensitivity for parallel acquisition in asynchronous cellular networks. IEEE Transactions on Wireless Communications 9(12), 3770–3778 (2010)
18. Li, X., Merrett, G.V., White, N.M.: Energy-efficient data acquisition for accurate signal estimation in wireless sensor networks. EURASIP Journal on Wireless Communications and Networking 13(18), 1–15 (2013)
19. Lin, J., Yin, S., Li, W.: Performance of combined saw convolver/serial-search acquisition for dsss system with single-tone jamming. In: International Conference on Communication Technology Proceedings. pp. 370–374. IEEE, Beijing (1996)
20. Liou, M., Chiueh, T.: A low-power digital matched filter for direct-sequence spread-spectrum signal acquisition. IEEE Journal of Solid-State Circuits 36(6), 933 – 943 (2001)
21. Madhow, U., Pursley, M.B.: Acquisition in direct-sequence spread-spectrum communication networks: An asymptotic analysis. IEEE Transactions on Information Theory 39(3), 903–912 (1993)
22. Mishali, M., Eldar, Y.C., Elron, A.J.: Xampling: Signal acquisition and processing in union of subspaces. IEEE Transactions on Signal Processing 59(10), 4719–4734 (2011)
23. Persson, B., Bolton, R.J.: A segmented matched filter for cdma code synchronization in systems with doppler frequency offset. In: IEEE Global Telecommunications Conference. pp. 648–653. IEEE, San Antonio (2001)
24. Puska, H., Sarnisaari, H., Iinatti, J., Lilj, P.: Serial search code acquisition using smart antennas with single correlator or matched filter. IEEE Transactions on Communications 56(2), 299–308 (2008)
25. Renzo, M.D., Annoni, L., Graziosi, F., Santucci, F.: A novel class of algorithms for timing acquisition of differential transmitted reference uwb receivers: Architecture, performance analysis and system design. IEEE Transactions on Wireless Communications 7(6), 2368–2387 (2008)
26. Sartipi, M., Fletcher, R.: Energy-efficient data acquisition in wireless sensor networks using compressed sensing. In: Data Compression Conference. pp. 223–232. IEEE, Snowbird (2011)
27. Sun, Z., Akyildi, I.F.: Magnetic induction communications for wireless underground sensor networks. IEEE Transactions on Antenna and Propagation 58(7), 2426–2435 (2010)
28. Tiansi, H., Yunsi, F.: Qelar: A machine-learning-based adaptive routing protocol for energy-efficient and lifetime extended underwater sensor networks. IEEE Transactions on Mobile Computing 9(6), 796–809 (2010)
29. Yamada, M., Kamio, Y., Wada, Y.: Acquisition of direct-sequence spread-spectrum signal with parallel matched filters. In: IEEE International Symposium on Personal, Indoor and Mobile Radio Communications. pp. 1260–1264. IEEE, London (2000)
30. Yang, J., Zhang, C., Li, X., Huang, Y., Fu, S., Acevado, M.F.: Integration of wireless sensor networks in environmental monitoring cyber infrastructure. Wireless Networks archive 16(4), 1091–1108 (2010)
31. Yen, N.Y., Su, S.L.: Robust matched-filter acquisition for direct-sequence ultrawideband systems. IEEE Transactions on Vehicular Technology 58(8), 4419 – 4425 (2009)

Wei Liang received his PHD in computing science from Hunan University, China, in 2013. He is currently a Associate Professor in College of Software Engineering, Xiamen University of Technology, China. His current research interests include vehicular networks, real-time embedded systems and field programmable gate arrays.

Yong Xie received his BE in computer science and technology from Hunan University of Science and Technology, China, in 2007, and PhD in computing science from Hunan University, China, in 2013. His research interests include real-time embedded systems, intellectual property protection, field programmable gate arrays, wireless sensor networks. Dr. Xie is the corresponding author of this paper.

Xuhui Chen received his PHD in computing science from Xi'an Jiaotong University, China, in 2003. He is currently a Professor in department of Software Engineering, Xiamen University of Technology, China. His current research interests include steganography, real-time embedded systems and field programmable gate arrays.

Osama Hosam received his PHD in computer science and technology from Hunan University of Science and Technology, China, in 2011. He is currently a assistant Professor College of the Computer Science and Engineering at Taibah University, Egypt. His research interests include real-time embedded systems, intellectual property protection, field programmable gate arrays, image watermarking.

Xiaoyan Chen received her MS in Department of Software Engineering from the Xiamen University, China, in 2012. His current research interests include real-time embedded systems, intellectual property protection, and field programmable gate arrays.

Received: February 24, 2016; Accepted: May 25, 2016.